MICROBIOLOGY

METHOD

Söderström *et al.*, *Microbiology*

DOI 10.1099/mic.0.000996

MICROBIOLOGY SOCIETY

An OregonGreen488-labelled D-amino acid for visualizing peptidoglycan by super-resolution STED nanoscopy

Bill Söderström[1,2]†, Alessandro Ruda[3]†, Göran Widmalm[3,*] and Daniel O. Daley[4,*]

Abstract

Fluorescent D-amino acids (FDAAs) are molecular probes that are widely used for labelling the peptidoglycan layer of bacteria. When added to growing cells they are incorporated into the stem peptide by a transpeptidase reaction, allowing the timing and localization of peptidoglycan synthesis to be determined by fluorescence microscopy. Herein we describe the chemical synthesis of an OregonGreen488-labelled FDAA (OGDA). We also demonstrate that OGDA can be efficiently incorporated into the PG of Gram-positive and some Gram-negative bacteria, and imaged by super-resolution stimulated emission depletion (STED) nanoscopy at a resolution well below 100 nm.

DATA SUMMARY

The authors confirm all supporting data, code and protocols have been provided within the article or through supplementary data files.

INTRODUCTION

The peptidoglycan (PG) layer is a continuous elastic mesh that surrounds the cytoplasmic membrane of bacteria [1]. It is a single layer thick in Gram-negative strains, but has a multi-layered structure in Gram-positive strains. Structures of the PG from the Gram-positive strains *Staphylococcus aureus* and *Bacillus subtilus*, obtained using atomic force microscopy, indicate that it is a non-homogeneous porous mesh that is tens of nanometres thick [2]. This mesh defines the shape of the bacterium and provides mechanical strength against the internal turgor pressure of the cell [3].

The PG layer is continually synthesized and remodelled so that bacterial cells can grow and subsequently divide (reviewed in [4]). These processes require the co-ordinated activities of PG hydrolyses (lytic transglycosylases, amidases, endopeptidases and carboxypeptidases) and PG synthases (glycosyltransferases, transpeptidases and bifunctional enzymes) [5]. The former open up the PG layer, whilst the latter insert a disaccharide of N-acetylglucosamine and N-acetylmuramic acid containing a short stem peptide. The disaccharide is polymerized into glycan strands and the stem peptides are cross-linked to create the layer. Maintaining the integrity of the PG layer is essential for cell viability, as cells lyse when it is compromised, for example, through the inhibition of PG synthases by ß-lactam antibiotics [6, 7].

Fluorescent D-amino acids (FDAAs) are molecular probes that are widely used to label the PG layer. They are integrated by D,D- and L,D-transpeptidases, which exchange free D-amino acids and FDAAs into position 4 (*Escherichia coli*) or 5 (*B. subtilus*) of the stem peptide [8]. Once integrated, they can be visualized by fluorescence microscopy. The VanNieuwenhze laboratory has developed more than 10 different types of FDAAs [9, 10], as well as rotor-fluorogenic versions (RFDAAs) [11]. This collection includes fluorophores that span the entire visible spectrum, providing options for multi-colour labelling and imaging of the PG by sequential addition of different FDAAs. The collection of FDAAs has been used to study the morphology and growth of the PG, to correlate sites

Received 09 September 2020; Accepted 10 November 2020; Published 25 November 2020

Author affiliations: [1]The iThree Institute, University of Technology Sydney, Australia; [2]Structural Cellular Biology Unit, Okinawa Institute of Science and Technology, Japan; [3]Department of Organic Chemistry, Stockholm University, Sweden; [4]Department of Biochemistry and Biophysics, Stockholm University, Sweden.

***Correspondence:** Göran Widmalm, Goran.Widmalm@su.se; Daniel O. Daley, ddaley@dbb.su.se

Keywords: FDAA; FLDA; OGDA; OregonGreen488; peptidoglycan; transpeptidase.

Abbreviations: *B. subtilis*, *Bacillus subtilis*; *E. coli*, *Escherichia coli*; FDAA, fluorescent D-amino acid; FLDA, fluorescein-labelled D-amino acid; NMR, nuclear magnetic resonance; OGDA, OregonGreen488-labelled D-amino acid; PG, peptidoglycan; *S. aureus*, *Staphylococcus aureus*; SIM, structured illumination microscopy; *S. mutans*, *Streptococcus mutans*; STED, stimulated emission depletion; TADA, TAMARA-labelled D-amino acid; *Z. mobilis*, *Zymomonas mobilis*.

†These authors contributed equally to this work

Four supplementary figures and one supplementary scheme are available with the online version of this article.

of PG synthesis with specific enzymes, to study PG turnover, and to determine the efficacy of antibiotics in perturbing PG synthesis (reviewed in [12]).

In recent years, super-resolution nanoscopy has emerged as a powerful technique for studying PG biosynthesis at the nanoscale. Two commonly used techniques are 3D structured illumination microscopy (3D-SIM) and stimulated emission depletion (STED) (reviewed in [13–15]). 3D-SIM can be used to reveal the dynamic and time-dependent processes, but only offers modest spatial resolution compared to other methods. STED imaging generally yields a higher spatial resolution but is typically limited to fixed samples, and is therefore not useful for studying dynamic processes. These methods have been used to probe the relative organization of fluorescently labelled proteins involved in cell division and PG biosynthesis [16–18]. Unfortunately, most FDAAs are not well suited for STED nanoscopy as the attached fluorophores do not possess the requisite photophysical properties. Only Atto488DA (green-shifted), Cy_{3B}DA and TADA (both yellow to orange shifted) could potentially be used [10], but they are not commercially available and have therefore not yet been extensively tested.

Herein we describe the synthesis and characterization of an OregonGreen488-labelled D-amino acid (OGDA). The OregonGreen488 fluorophore has an excitation maximum of 501 nm and an emission maximum of 526 nm. It was chosen because it has a high extinction coefficient and fluorescence quantum yield, making it one of the best performing dyes for STED nanoscopy [19]. A fluorescein-labelled D-amino acid (FLDA) was also synthesized and used for comparison to the STED imaging with OGDA. The fluorescein fluorophore has an excitation maximum of 494 nm and emission maximum of 512 nm. It is more suitable for confocal fluorescence microscopy as it lacks the proper photostability characteristics for STED nanoscopy.

Impact Statement

Herein we describe the synthesis and characterization of a D-amino acid conjugated to the OregonGreen488 fluorophore (which we have named OGDA). We demonstrate that OGDA is incorporated into the peptidoglycan layer of Gram-positive, and some Gram-negative, bacteria. Since the OregonGreen488 fluorophore has suitable photophysical properties, OGDA can be imaged by super-resolution nanoscopy. OGDA is compatible with other fluorescent D-amino acids and will be a valuable resource for studying peptidoglycan biosynthesis, inhibition of peptidoglycan biosynthesis by antibiotics, and peptidoglycan turnover.

THEORY AND IMPLEMENTATION

Synthesis of two novel FDAAs

Two novel FDAAs were synthesized using a suitably protected D-alanine analogue, namely, N^{α}-Boc-D-2,3-diaminopropionic acid, reacting with *N*-hydroxysuccinimide esters of either fluorescein (as a mixture of positional isomers) or OregonGreen488 (Scheme S1, available in the online version of this article). The coupling was performed under basic conditions using previously developed experimental procedures [10, 20] followed by deprotection of the *tert*-butoxycarbonyl group with acid and finally purification on a short reversed-phase C18 column. The fluorescein-labelled D-alanine is hereafter referred to as FLDA, and the OregonGreen488-labelled D-alanine is referred to as OGDA.

Incorporation of FDAAs into the peptidoglycan of Gram-positive bacteria

We tested whether three Gram-positive strains could incorporate FLDA and OGDA into their PG. Exponentially growing *Streptococcus mutans*, *S. aureus* and *B. subtilis* were labelled with 1 mM of either FLDA or OGDA for 1–5 min. This labelling time roughly corresponded to between 2% (*S. mutans*, *S. aureus*) and 20% (*B. subtilis*) of the cell cycle. Cells were then washed, fixed and imaged by confocal microscopy so that regions of incorporation into the PG layer could be visualized. We observed that both FLDA and OGDA were incorporated into the division site in nearly all cells (Fig. 1a, b). This observation was anticipated, as this is where PG synthesis is predominantly occurring [10, 20]. These data indicate that both FLDA and OGDA are efficiently incorporated into newly synthesized PG of Gram-positive bacteria and that they can be imaged by confocal microscopy.

We also imaged the same cells with super-resolution STED nanoscopy [21]. As anticipated, FLDA was challenging to image (Fig. 1a), because the photophysical properties of fluorescein are not optimal for super-resolution microscopy. In contrast, OGDA was relatively easy to image (Fig. 1b), as the OregonGreen488 fluorophore is highly resistant to bleaching and extremely photo-stable [19]. Quantification of fluorescence intensities from raw STED images indicated that ODGA was on average twice as bright as FLDA (Fig. 1c). To assess the resolution that could be obtained using OGDA, the STED images of *S. mutans* were further analysed. Here the minimal resolvable peak-to-peak distance of fluorescence maxima at the division site of OGDA-labelled cells was estimated to be approximately 85 nm (Fig. 2). It is anticipated that this number will vary from experiment to experiment. Nevertheless, it unequivocally shows that it is viable to use OGDA to image PG incorporation using super-resolution nanoscopy.

We carried out a virtual time lapse in *S. mutans* with OGDA and the yellow to orange shifted TADA [10]. This enabled us to capture the history of PG synthesis at the division site over time. In this experiment *S. mutans* cells were first pulse-labelled with OGDA, and then with TADA at intervals of 10 min (Fig. 3a). We observed that the OGDA was initially inserted into the PG at the division site, but was subsequently pushed away from the division site as new TADA-labelled PG was synthesized, resulting in a stripe

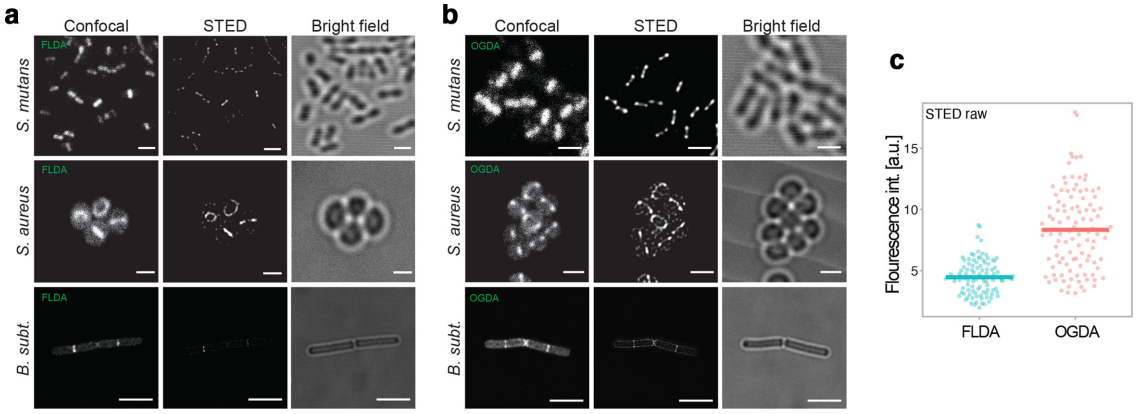

Fig. 1. Confocal and STED microscopy images of (a) fluorescein-containing D-amino acid (FDAA) and (b) OregonGreen488-containing D-amino acid (OGDA) in various Gram-positive strains. Scale bar, 4 µm. (c) The relative fluorescence intensity at the division septum of *S. mutans* labelled with OGDA was twice that of FLDA; n_{FLDA}=110, n_{OGDA}=106.

pattern (Fig. 3b). If cells were in a very late phase of division when the labelling was initiated, TADA was also incorporated into the division sites of the daughter cells (Fig. 3c).

As STED is a relatively complex microscopy approach and not yet accessible to many researchers, we also imaged cells by super-resolution structured illumination microscopy (SIM), a technique that is more broadly accessible (Fig. 3d). Finally, we also reversed the labelling sequence, with TADA first and OGDA last, to ensure that the order of the labelling did not influence the outcomes. As expected, we observed similar results, but with an inverted colour pattern (Fig. S1). Taken together, these data indicate that OGDA is compatible with TADA for super-resolution imaging using both STED and SIM [10].

Incorporation of FDAAs into the peptidoglycan of Gram-negative bacteria

It has previously been documented that most FDAAs do not work in Gram-negative bacteria because they cannot cross the outer membrane [11, 12]. This membrane acts as a permeability barrier to most chemical compounds, in particular those that are larger than 500–600 Da [22]. As OGDA is 498 Da, we tested whether it could be incorporated into the model Gram-negative bacterium *E. coli*

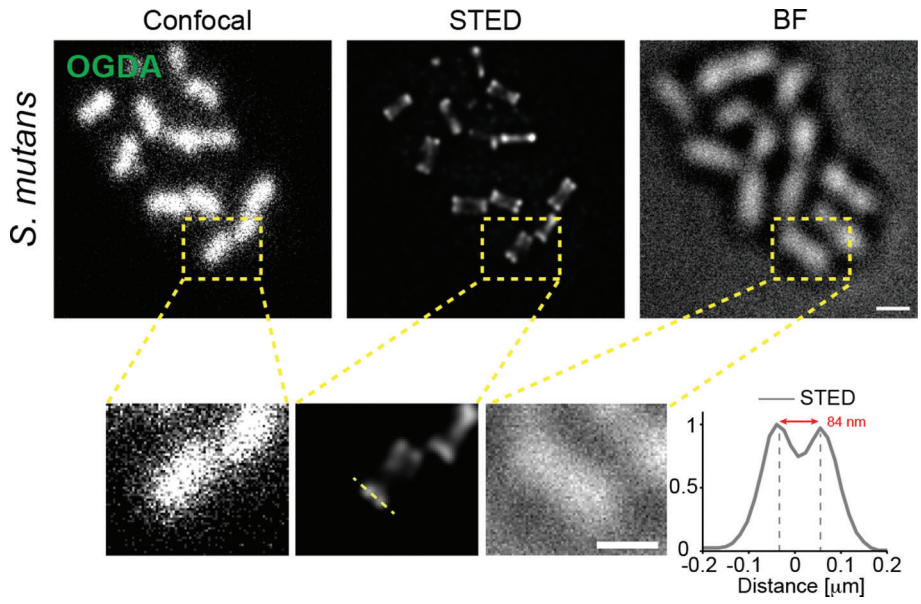

Fig. 2. Confocal and STED images of a *S. mutans* cell labelled with OGDA. The fluorescence intensity was measured by drawing a line over the OGDA signal along the long axis of the cell. The graph shows the OGDA fluorescence intensity trace over the septum (yellow dotted line on the STED image). The peak-to-peak distance was ~85 nm. Scale bar, 500 nm.

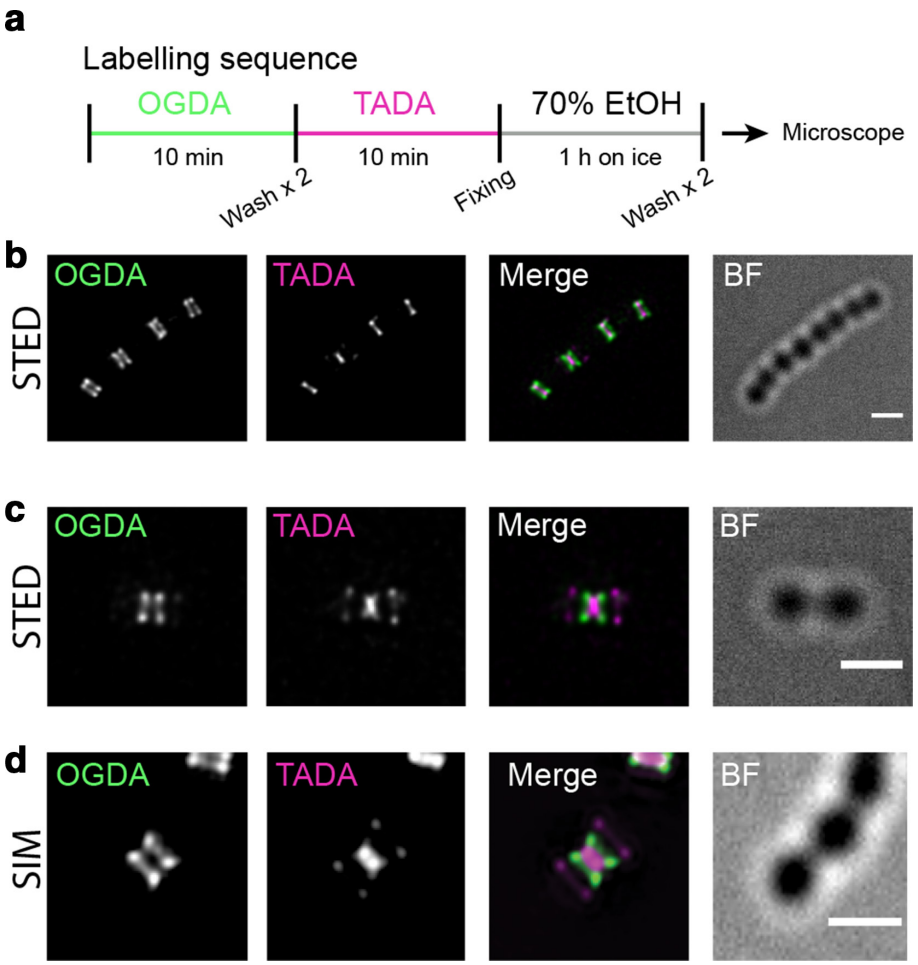

Fig. 3. Virtual time lapse imaging during two-colour FDAA labelling. (a) *S. mutans* cells were pulse-labelled with OGDA for 10 min, washed, labelled with TADA for 10 min, and finally fixed in ethanol for 1 h. (b) Typical stripe pattern resulting from the labelling scheme. ODGA is pushed away from the division site as new TADA-labelled PG is synthesized. (c) If the first labelling (of the first FDAA, e.g. OGDA) occurs late in the division cycle, the second FDAA will label both the old septum and part of the future division site, indicating that PG synthesis could be ongoing at both places at the same time. (d) To make sure that the OGDA could have a broader use, cells were also imaged by structural illumination microscopy (SIM). Scale bar, 1 µm.

(MG1655). In this series of experiments, cells were labelled with 1 mM of OGDA for 5 min, which corresponds to less than 20% of the cell cycle. Cells were then washed, fixed and imaged by confocal microscopy and STED so that regions of incorporation into the PG layer could be visualized. Although we observed fluorescence at the division site of some cells (Fig. 4a), the vast majority of cells were not labelled (data not shown). We also tested whether a strain lacking the glycosyltransferase WaaG (Δ*waaG*) was more permeable to OGDA. This strain is a 'deep rough' lipopolysaccharide mutant that is considered 'leaky', as it is hyper-sensitive to antibiotics such as novobiocin (612 Da) erythromycin (733 Da), rifampicin (823 Da) and vancomycin (1449 Da) [23]. However, we did not observe increased incorporation of OGDA (data not shown). We did, however, observe incorporation of OGDA in *Zymomonas mobilis,* a Gram-negative bacterium that is used for industrial production of ethanol (Fig. 4b). Here we observed that >95% of all cells were labelled at the division site after 5 min with 1 mM OGDA. Even though this labelling time corresponded to less than 5% of the cell cycle, many of the cells were also labelled in the perimeter of the membranes (Fig. S2).

CONCLUSION

Herein we describe the synthesis of two new FDAAs in the green spectrum: OregonGreen488–FDAA (OGDA) and fluorescein–FDAA (FLDA). Like FDAAs that have been described previously, they are integrated into the PG layer and can be visualized by fluorescence microscopy [9, 10]. They can therefore be used as molecular probes for localizing sites of peptidoglycan biosynthesis, for determining how antibiotics inhibit peptidoglycan biosynthesis and for studying peptidoglycan turnover.

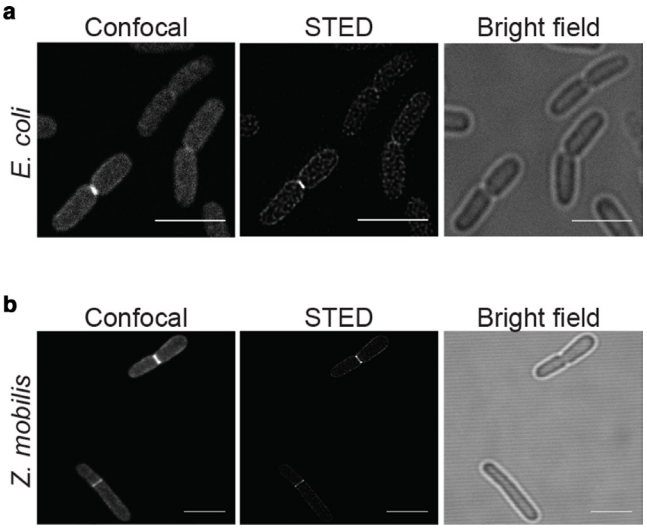

Fig. 4. OGDA labelling and STED imaging of Gram-negative bacteria. (a) Poorly labelled *E. coli* cells. (b) *Z. mobilis* cells were labelled more efficiently; it can be seen that in *Z. mobilis* cells the division machinery is not always placed at midcell and that PG synthesis is ongoing early in the constriction process (i.e. before visible constriction). Scale bar, 2 µm.

Notably, OGDA is suitable for super-resolution STED nanoscopy as the OregonGreen488 fluorophore is resistant to bleaching and extremely photo-stable [19]. We used OGDA and STED to image sites of PG insertion at a resolution of ~85 nm. Moreover, we demonstrated that OGDA could be used in parallel with the orange-shifted TADA for dual-colour STED imaging. In principle, OGDA should also be compatible with the orange-shifted Cy_{3B}ADA for STED imaging [10]. The availability of OGDA and STED to study PG insertion will help researchers to more accurately pinpoint sites of PG insertion in time and space, and determine whether given PG synthesizing proteins co-localize at these sites. This may help to address a number of open questions in bacterial cell wall synthesis.

Although OGDA worked in all in Gram-positive strains tested, it may have limited used in Gram-negative bacteria. We noted that it was incorporated into the PG layer of *Z. mobilis*, but that it was not efficiently incorporated into the PG layer of the *E. coli* strains we tested. This is most likely because the molecular weight of OGDA (498 Da) is close to the molecular weight cut-off for porins in the outer membrane in *E. coli* (500–600 Da) [22]. This problem has been noted for most FDAAs [11, 12].

METHODS

General

NHS–fluorescein (5/6-carboxyfluorescein succinimidyl ester), mixed isomer, OregonGreen488 carboxylic acid, succinimidyl ester, 6-isomer and N^{α}-Boc-D-2,3-diaminopropionic acid were purchased from Thermo Fisher Scientific (Kandel, Germany). Dry acetonitrile (ACN) was purchased from Honeywell Research Chemicals (Bucharest, Romania), and dry *N*,*N*-dimethylformamide (DMF) and dichloromethane (DCM) were purchased from Acros Organics (Morris Plains, NJ, USA). *N*,*N*-diisopropylethylamine (DIPEA) was purchased from Sigma-Aldrich (Geel, Belgium). All reagents were used as received. A nitrogen flow was used for reactions requiring inert atmosphere. Purification was performed on Sep-Pak C18 Plus short cartridges, 55–105 µm particle size (Waters, Milford, MA, USA). MQ water was obtained from the Elga Purelab Ultra Genetic Water Purification System (High Wycombe, UK). One-dimensional ^{1}H and ^{13}C, and 2D multiplicity-edited ^{1}H,^{13}C-HSQC nuclear magnetic resonance (NMR) spectra for the characterization of isolated compounds were recorded in MeOH-d_4 at 298 K on a Bruker AVANCE III 700 MHz equipped with a 5 mm TCI Z-Gradient Cryoprobe (^{1}H/^{13}C/^{15}N), a Bruker AVANCE III 600 MHz spectrometer equipped with a 5 mm TXI inverse Z-Gradient ^{1}H/D-^{31}P/^{13}C and a Bruker AVANCE III HD 400 MHz spectrometer equipped with a 5 mm BBF/H/D 5.0 Z probe. The NMR chemical shifts (δ) are reported in p.p.m. and referenced to residual methanol δ_H 3.31, internally to the MeOD-d_4 solvent peak, δ_C 49.00, or externally to fluorobenzene, δ_F −115.42, in MeOD [24]. *J* coupling constants are reported in hertz (Hz). High-resolution mass spectra (HRMS) were recorded on Bruker Daltonics micrOTOF or micrOTOFQ spectrometers (Bremen, Germany) using electrospray ionization (ESI) in the positive mode. Samples for mass spectrometry (MS) were prepared using a solution of acetone and H_2O in a 1 : 1 ratio.

Synthesis of fluorescently labelled D-amino acid

Fluorescent dye was allowed to attain room temperature (RT) before the vial was opened. To a flame-dried 5 ml flask succinimidyl ester dye derivative (5 mg, 1 eq) and N^{α}-Boc-D-2,3-diaminopropionic acid (1.4 eq) were added under nitrogen flow. Dry DMF (0.2 ml) and freshly distilled DIPEA (2.5 µl) were then added and the reaction was left under stirring for 2 h while being monitored by HRMS. Thereafter, the reaction mixture was co-evaporated under vacuum with dry toluene (40 °C).

Removal of the Boc protecting group was achieved by treatment with DCM/TFA (1 : 1, 2 ml) for 30 min at RT. The crude, concentrated under reduced pressure, was redissolved in MQ water (0.5 ml) and few drops of ACN and passed through a Sep-Pak C18 Plus short cartridge that had been pre-equilibrated with MQ-water (10 ml) and ACN (10 ml), using in sequence MQ water (5 ml), water/ACN (9 : 1, 5 ml), water/ACN (7 : 3, 5 ml) and ACN (5 ml). Fractions collected were checked by MS, pooled and freeze-dried twice to yield an orange/red powder.

Analytical data

Fluorescein D-amino acid (FDAA)

(*R*)-2-amino-3-(3′,6′-dihydroxy-3-oxo-3*H*-spiro[isobenzofuran-1,9′-xanthene]-5-carboxamido) propanoic acid and **(*R*)-2-amino-3-(3′,6′-dihydroxy-3-oxo-**

3*H*-spiro[isobenzofuran-1,9′-xanthene]-6-carboxamido) propanoic acid

^{1}H NMR (700 MHz, MeOD, 298 K): δ 8.52 (dd, 1H, ^4J 1.6 Hz, ^5J 0.7 Hz, I1), 8.23 (dd, 1H, ^3J 8.0 Hz, ^4J 1.6 Hz, I1), 8.18 (dd, 1H, ^3J 8.1 Hz, ^4J 1.5 Hz, I2), 8.12 (dd, 1H, ^3J 8.1 Hz, ^5J 0.7 Hz, I2), 7.71 (dd, 1H, ^4J 1.5 Hz, ^5J 0.7 Hz, I2), 7.34 (dd, 1H, ^3J 8.0 Hz, ^5J 0.7 Hz, I1), 6.77–6.69(4H, Ar), 6.61–6.57 (2 H, Ar), 4.00 (1H, H_β, I1), 3.90 (1H, H_β, I1/I2), 3.88 (1H, H_β, I1/I2), 3.87 (1H, H_α, I1), 3.77(1H, H_β, I2), 3.75(1H, H_α, I2). ^{13}C NMR (175 MHz, MeOD, 298 K) selected data: δ 172.9, 172.8, 171.9, 171.8, 170.8, 170.7 (6×C=O), 156.0, 141.2 (2×quat), 137.8, 135.3, 131.7, 131.5, 128.0, 127.7, 127.0, 126.3, 116.3, 112.8, 104.6, 58.1, 58.0 (2×C_α), 43.1, 42.9 (2×C_β). ESI-HRMS: $[M-H]^-$*m/z* calculated for $C_{24}H_{17}N_2O_8$ 461.0967, found 461.0990. Yield: 78 %. Isomeric ratio between major (of intensity I1) and minor (of intensity I2) product: ~2 : 1. See Fig. S3.

OregonGreen488 D-amino acid (OGDA) (*R*)-2-amino-3-(2′,7′-difluoro-3′,6′-dihydroxy-3-oxo-3*H*-spiro[isobenzofuran-1,9′-xanthene]-6-carboxamido) propanoic acid

^{1}H NMR (600 MHz, MeOD, 298 K): δ 8.21 (dd, 1H, ^3J 8.1 Hz, ^4J 1.5 Hz, Ar-H), 8.17 (dd, 1H, ^3J 8.1 Hz, ^5J 0.7 Hz, Ar-H), 7.73 (dd, 1H, ^4J 1.5 Hz, ^5J 0.7 Hz), 6.873 (d, 1H, $^4J_{F,H}$ 7.3 Hz), 6.872 (d, 1H, $^4J_{F,H}$ 7.3 Hz), 6.52 (d, 1H, $^3J_{F,H}$ 11.1 Hz), 6.51 (d, 1H, $^3J_{F,H}$ 11.1 Hz), 3.90 (1H, H_β), 3.77 (1H, H_β), 3.76 (1H, H_α). ^{13}C NMR (150 MHz, MeOD, 298 K) selected data: δ 172.7, 170.8, 170.6 (3×C=O), 152.2, 151.4, 150.6, 142.2 (4×quat), 131.7, 128.1, 125.9, 115.4 (d, $^2J_{C,F}$ 21 Hz), 115.3 (d, $^2J_{C,F}$ 21 Hz), 111.3 (quat), 107.0, 57.9 (C_α), 42.8 (C_β). ^{19}F NMR (376 MHz, MeOD, 298 K): δ −141.3 (C_{Ar}-F). ESI-HRMS: $[M-H]^-$*m/z* calculated for $C_{24}H_{15}N_2O_8F_2$ 497.0802, found 497.0787. Yield: 81%. See Fig. S4.

Bacterial growth

S. mutans (UA159) was grown in THYE (Todd Hewitt broth+0.3% yeast extract) media under anaerobic conditions without shaking at 37 °C. *S. aureus* (RN4220) was grown in tryptic soy broth (TSB) media with shaking (200 r.p.m.) at 37 °C. *B. subtilis* (PY79) was grown in half Lennox broth (LB) media with shaking (200 r.p.m.) at 30 °C. *Z. mobilis* (ZM6) was grown in complex medium (20 g l^{-1} glucose, 5 g l^{-1} yeast extract, 1 g l^{-1} KH_2PO_4, 1 g l^{-1} $(NH_4)_2SO_4$, 0.5 g l^{-1} $MgSO_4$) with shaking (200 r.p.m.) at 37 °C. *E. coli* (MG1655) was grown in LB media with shaking (200 r.p.m.) at 37 °C. Cultures grown overnight were back-diluted 1 : 200 and subsequently allowed to grow to an OD_{600} of 0.3–0.5 before FDAA labelling.

FDAA labelling

A stock solution (100 mM in DMSO) of FDAA was kept at −80 °C until use. All strains were labelled with 1 mM of corresponding FDAA. Gram-negative species (*E. coli* and *Z. mobilis*) were labelled for 5 min, while Gram-positive species (*S. mutans, S. aureus* and *B. subtilis*) were labelled for 1–2 min and then fixed with 90% ice-cold methanol or 70% ice-cold ethanol, as described [20]. For virtual time lapse labelling (Fig. 4) the protocol devised by Hsu *et al.* [10] was followed with minor adjustments. *S. mutans* were grown as described above; at OD_{600}~0.5 the cultures were labelled with 1 mM of either OGDA or TADA [25] and left to grow for 10 min without shaking at 37 °C. Cultures were pelleted (9000 ***g***, 3 min), washed twice in pre-warmed THYE media and then labelled with the second FDAA (either OGDA or TADA) for another 10 min without shaking at 37 °C. The cultures were then fixed with 70% ice-cold ethanol and incubated on ice for ~1 h. Lastly, the cultures were washed twice in phosphate-buffered saline (PBS) at 4 °C. Labelled cells were applied on a premade agarose pad [2% agarose (w/v)] and imaged within 2 h.

Imaging

Gated STED (gSTED) images were acquired on a Leica TCS SP8 STED 3× system in a similar way to that described by Söderström *et al.* [18] using a HC PL Apo 100× oil immersion objective with NA 1.40. OregonGreen488 was excited using a white laser operated at 488 nm. A STED laser line operated at 592 nm was used as a depletion laser. A detection time delay of 1.3 ns was applied. The total depletion laser intensity was in the order of 40 MW cm^{-2} for all STED imaging. The final pixel size was 24 nm and the scanning speed was 600 Hz. The pinhole size was set to 0.9 AU.

SIM images were acquired using a Zeiss ELYRA PS1 equipped with a pco.edge sCMOS camera and 100×1.46 NA plan Apo oil immersion objective. The final pixel size in SIM images was 25 nm. Individual images were acquired using an acquisition time of 500 ms^{-1} image (a total of 25 images were acquired per SIM image reconstruction) and subsequently reconstructed from the raw data using ZEN2012 software [26].

Image analysis and post processing

Images were subsequently transferred to ImageJ/Fiji for figure preparation. Line traces were drawn over the FDAA-labelled septum along the long axis of the cells. Graphs were assembled in Origin Pro 9, and the minimal resolvable peak-to-peak distance was measured and taken as an indication of achieved resolution (~85 nm). The integrated fluorescence intensity was measured over the septum of non-dividing cells and subsequently plotted using the open software PlotsOfData [27].

Funding information
D. O. D. was supported by grants from the Swedish Research Council and Carl Trygger Stiftelse för Vetenskaplig Forskning. B. S. was supported by a Young Scientist grant from JSPS Kakenhi, Japan (JP17K15694) and a CPDRF grant from the University of Technology Sydney. Work in the SCB unit at OIST is funded by a core subsidy from Okinawa Institute of Science and Technology. G. W. was supported by grants from the Swedish Research Council (no. 2017–03703) and The Knut and Alice Wallenberg Foundation.

Acknowledgements
We would like to thank Dr Patricia Lara (University of Florida) for the *S. mutans* strain, Dr Katsuya Fuchino (Norwegian Institute of Science and Technology) for the *Z. mobilis* strain and Dr Helena Chan (Okinawa Institute of Science and Technology) for the *S. aureus* strain.

Author contributions
B. S. and D. O. D. conceived the study. B. S. and A. R. performed the experiments. All authors analysed the data and wrote the manuscript.

Conflicts of interest
The authors declare that there are no conflicts of interest.

References

1. Vollmer W, Blanot D, de Pedro MA. Peptidoglycan structure and architecture. *FEMS Microbiol Rev* 2008;32:149–167.
2. Pasquina-Lemonche L, Burns J, Turner RD, Kumar S, Tank R *et al*. The architecture of the Gram-positive bacterial cell wall. *Nature* 2020;582:294–297.
3. Xiao J, Goley ED. Redefining the roles of the FtsZ-ring in bacterial cytokinesis. *Curr Opin Microbiol* 2016;34:90–96.
4. Egan AJF, Errington J, Vollmer W. Regulation of peptidoglycan synthesis and remodelling. *Nat Rev Microbiol* 2020;18:446–460.
5. Pazos M, Peters K, Vollmer W. Robust peptidoglycan growth by dynamic and variable multi-protein complexes. *Curr Opin Microbiol* 2017;36:55–61.
6. Chung HS, Yao Z, Goehring NW, Kishony R, Beckwith J *et al*. Rapid beta-lactam-induced lysis requires successful assembly of the cell division machinery. *Proc Natl Acad Sci U S A* 2009;106:21872–21877.
7. Yao Z, Kahne D, Kishony R. Distinct single-cell morphological dynamics under beta-lactam antibiotics. *Mol Cell* 2012;48:705–712.
8. Kuru E, Radkov A, Meng X, Egan A, Alvarez L *et al*. Mechanisms of incorporation for D-amino acid probes that target peptidoglycan biosynthesis. *ACS Chem Biol* 2019;14:2745–2756.
9. Kuru E, Hughes HV, Brown PJ, Hall E, Tekkam S *et al*. In Situ probing of newly synthesized peptidoglycan in live bacteria with fluorescent D-amino acids. *Angew Chem Int Ed Engl* 2012;51:pp:12519–12523.
10. Hsu Y-P, Rittichier J, Kuru E, Yablonowski J, Pasciak E *et al*. Full color palette of fluorescent D-amino acids for *in situ* labeling of bacterial cell walls. *Chem Sci* 2017;8:6313–6321.
11. Hsu Y-P, Hall E, Booher G, Murphy B, Radkov AD *et al*. Fluorogenic D-amino acids enable real-time monitoring of peptidoglycan biosynthesis and high-throughput transpeptidation assays. *Nat Chem* 2019;11:335–341.
12. Hsu Y-P, Booher G, Egan A, Vollmer W, VanNieuwenhze MS. D-Amino acid derivatives as in situ probes for visualizing bacterial peptidoglycan biosynthesis. *Acc Chem Res* 2019;52:2713–2722.
13. Sahl SJ, Hell SW, Jakobs S. Fluorescence nanoscopy in cell biology. *Nat Rev Mol Cell Biol* 2017;18:685–701.
14. Coltharp C, Xiao J. Superresolution microscopy for microbiology. *Cell Microbiol* 2012;14:1808–1818.
15. Xiao J, Dufrêne YF. Optical and force nanoscopy in microbiology. *Nat Microbiol* 2016;1:16186.
16. Bisson-Filho AW, Hsu Y-P, Squyres GR, Kuru E, Wu F *et al*. Treadmilling by FtsZ filaments drives peptidoglycan synthesis and bacterial cell division. *Science* 2017;355:739–743.
17. Yang X, Lyu Z, Miguel A, McQuillen R, Huang KC *et al*. GTPase activity-coupled treadmilling of the bacterial tubulin FtsZ organizes septal cell wall synthesis. *Science* 2017;355:744–747.
18. Söderström B, Chan H, Shilling PJ, Skoglund U, Daley DO. Spatial separation of FtsZ and FtsN during cell division. *Mol Microbiol* 2018;107:387–401.
19. Beater S, Holzmeister P, Pibiri E, Lalkens B, Tinnefeld P. Choosing dyes for cw-STED nanoscopy using self-assembled nanorulers. *Phys Chem Chem Phys* 2014;16:6990–6996.
20. Kuru E, Tekkam S, Hall E, Brun YV, Van Nieuwenhze MS. Synthesis of fluorescent D-amino acids and their use for probing peptidoglycan synthesis and bacterial growth in situ. *Nat Protoc* 2015;10:33–52.
21. Vicidomini G, Moneron G, Han KY, Westphal V, Ta H *et al*. Sharper low-power STED nanoscopy by time gating. *Nat Methods* 2011;8:571–573.
22. Nikaido H. Molecular basis of bacterial outer membrane permeability revisited. *Microbiol Mol Biol Rev* 2003;67:593–656.
23. Muheim C, Götzke H, Eriksson AU, Lindberg S, Lauritsen I *et al*. Increasing the permeability of Escherichia coli using MAC13243. *Sci Rep* 2017;7:17629.
24. Rosenau CP, Jelier BJ, Gossert AD, Togni A. Exposing the origins of Irreproducibility in fluorine NMR spectroscopy. *Angew. Chem. Int. Ed.* 2018;57:pp:9528–9533.
25. Boersma MJ, Kuru E, Rittichier JT, VanNieuwenhze MS, Brun YV *et al*. Minimal peptidoglycan (PG) turnover in wild-type and PG hydrolase and cell division mutants of *Streptococcus pneumoniae* D39 growing Planktonically and in Host-Relevant biofilms. *J Bacteriol* 2015;197:3472–3485.
26. Söderström B, Badrutdinov A, Chan H, Skoglund U. Cell shape-independent FtsZ dynamics in synthetically remodeled bacterial cells. *Nat Commun* 2018;9:4323.
27. Postma M, Goedhart J. PlotsOfData-A web APP for visualizing data together with their summaries. *PLoS Biol* 2019;17:e3000202.